

STRIKE-POINT CHARACTERISTICS OF THE MAST TOKAMAK IN AUXILIARY HEATED PLASMAS

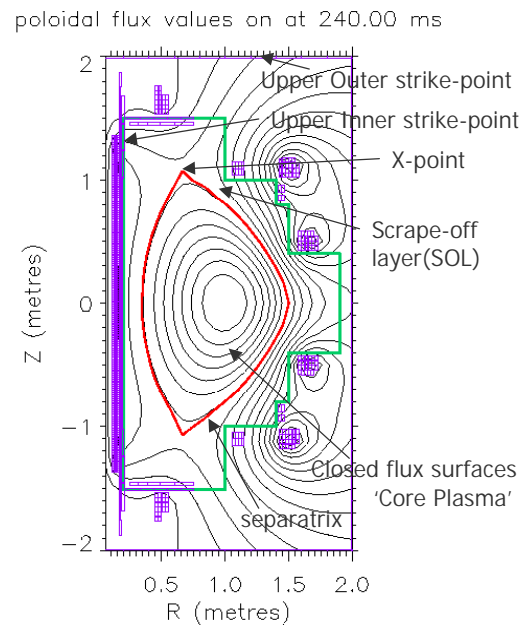
J-W. Ahn^a, G.F. Counsell, A. Kirk

Euratom/UKAEA Fusion Association, Culham Science Centre, Abingdon, Oxon OX14 3DB, UK

^aDepartment of Physics, Imperial College, University of London, London SW7 2BZ, UK

1. Introduction

Target plasma behaviour and the power loading problem are even more important in spherical tokamaks (STs) because of their smaller wetted areas, particularly on the inboard side. The Mega Ampere Spherical Tokamak (MAST) has been newly commissioned and has been operational since December 1999. The plasma performance so far includes up to 1 MA of plasma current, significant NBI auxiliary heating and clear access to H-mode. Initial observations[1] of plasma conditions, including power loading, at each of the four strike-points in MAST Double Null Divertor (DND) have been reported for a number of Ohmic plasmas, with flat top currents of about 500 kA and average electron density of around 10^{19} m^{-3} . A total of 192 Langmuir probes in 10 arrays are used as a main diagnostic tool to measure edge plasma parameters with a time resolution of around 3ms. The probes are spaced 3mm apart at the inboard side and 10mm at the outboard.



Shot number :2700

Fig.1 EFIT reconstruction image of a MAST DND discharge. The strike-points are the region of separatrix intersection with the material surfaces

2. Experimental Results

Target plasma parameter measurements for Ohmic discharges have now been supplemented by more detailed measurements in auxiliary heated L and H-mode DND plasmas. A typical MAST pulse length is currently ~ 300 ms and only data taken after the formation of a clear DND configuration (Fig.1), with the inboard separatrix well separated from the centre column, were analysed. Exponential curves are fitted to the probe I-V characteristics allowing derivation of T_e and other subsequent plasma parameters such as n_e and heat flux density q . The ion saturation current density, j_{sat} , indicates a direct measurement of the particle flux density. Only the region from ion saturation to just beyond floating potential was chosen for

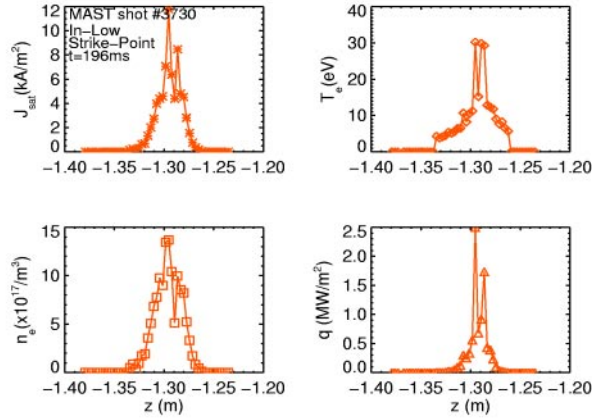


Fig.2 An example of the spatial variation of the target plasma parameters. This example shows possible evidence of double strike-points corresponding to the primary and parasitic separatrixes, ie in disconnected double null (DDN) configuration

off. Similar sets of data were obtained for each of the other three strike-points. The double peaks in each profile may be the result of two separatrixes hitting the divertor surfaces, caused by slight magnetic asymmetry resulting in disconnected double null (DDN) configuration. The EFIT equilibrium reconstruction code confirms that the plasma had two separatrixes at the corresponding time slice. This is also observed from the IR image viewing the outer lower divertor plate (Fig. 3).

Densities and temperatures for the inboard and outboard SOL correspond to collisional conditions in both L and H-mode phases. ($v_e^* = L/\lambda_{ee}$, where L is the parallel connection length, $\sim 30\text{m}$ at outboard and $\sim 20\text{m}$ at inboard, and λ_{ee} is the electron-electron mean free path.) It is interesting to note that the collisionality at the target ($v_e^* > 12$ from Langmuir probe data) is much higher than at the midplane ($v_e^* > 3$ from DIVIMP modelling [2]). The average collisionality along the flux tube is around $v_e^* > 6$. For a typical 0.75MW NBI heated shot such as 2951

(average $n_e^{core} \sim 2.5 \times 10^{19} \text{m}^{-3}$), density at the inboard strike-point ($n_{e,st}^{in} \sim 1.1\text{-}3.0 \times 10^{18} \text{m}^{-3}$) is significantly higher (and rises more quickly with core density) than at the outboard ($n_{e,st}^{out} \sim 3.0\text{-}8.5 \times 10^{17} \text{m}^{-3}$), though only by a factor ~ 3.5 compared with ~ 6 in the Ohmic case. The increase in $n_{e,st}^{in}$ with core density is accompanied by a rise in strike-point electron temperature, $T_{e,st}^{in}$, from $\sim 12\text{eV}$ to $\sim 30\text{eV}$ and a narrowing of the SOL temperature width at the target from $\sim 3.5\text{cm}$ to $\sim 1\text{cm}$, beginning after the transition to H-mode. This gives rise to a strong increase, during H-mode, in peak heat flux density at the inboard strike-point from $\sim 500\text{kWm}^{-2}$ to nearly 3MWm^{-2} (Fig.4), coupled with a rise in total power to all strike-points, P_{tar} , although the average P_{tar} in H-mode remains lower than in L-mode (Fig.5). The strike-point electron temperature at the outboard side, $T_{e,st}^{out}$, remains fairly constant (8-12eV)

analysis, in order to avoid distortion of the characteristic resulting from early saturation of electron current. The geometric probe area was used for obtaining n_e and q , instead of its projection perpendicular to the local field, to allow for the effect of large ion Larmor radii experienced in the relatively low field of MAST ($< 0.3\text{T}$ on the outboard side). Fig. 2 shows a typical example of the j_{sat} , T_e , n_e and q profiles across the lower inner strike-point, showing a clear exponential fall-



Fig.3 An IR image of outer-lower strike-point showing two separatrixes

although the electron density and heat flux density scale lengths fall by a factor three (from $\sim 12\text{cm}$ to $\sim 4\text{cm}$ and $\sim 9\text{cm}$ to $\sim 3\text{cm}$ respectively at the target) with transition to H-mode.

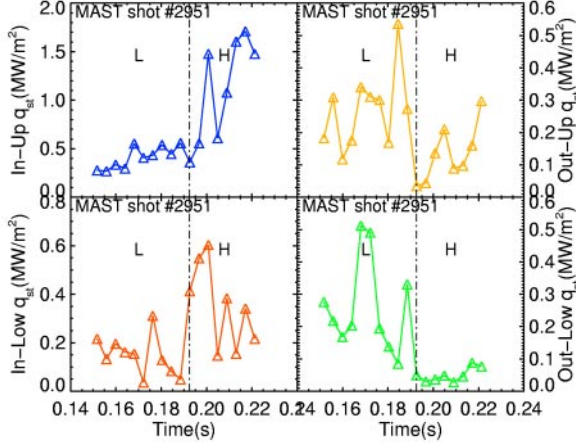


Fig.4 Temporal evolution of heat flux density at all strike points across the L-H transition

although the core density rapidly increases after the L-H transition. The inner P_{tar} increase in H-mode is obviously much steeper than the outer P_{tar} . The total power efflux into the SOLs,

P_{SOL} , is derived from $P_{SOL} \approx P_{Ohmic} - \frac{d}{dt}W + P_{NBI} - P_{RAD}$ assuming all the NBI power is absorbed

(reasonable at these densities) and a 40% core radiated power fraction (P_{RAD}). The rate of change of stored magnetic and thermal energy, dW/dt , is derived from the magnetic reconstruction code EFIT. The temporal variation of P_{tar} and the ratio of P_{tar}^{out} to P_{tar}^{in} as well as other relevant parameter variations are given in the Fig 5. The ratio of P_{tar} to P_{SOL} decreases

from $\sim 50\%$ to $\sim 10\%$, during the L-mode phase, with the average value of $\sim 33\%$ whereas it steadily increases in H-mode plasma up to around 35%. In both L and H-mode, the ratio is significantly lower than the $\sim 65\%$ observed for Ohmic plasmas [1]. Since there seems to be no relationship between P_{tar} and the core confinement (virtually no change in P_{SOL} observed across the L-H transition, see Fig 5), the cause of the missing power may be in the SOL itself. The additional power discrepancy between Ohmic and NBI heated plasmas may be associated with an increase in power

3. Power accounting

The total power flows to the targets, P_{tar} , were determined by integrating over the total surface area of the strike point region using the derived exponential profiles for the power density in both the SOL and private flux region (PFR), $P_{tar} = 2\pi R q_{st} (\lambda_q^{SOL} + \lambda_q^{PFR})$, where R = radius of strike point at target, q_{st} = heat flux density at the strike point and λ_q = heat flux density scale length. Figure 5 shows P_{tar} in H-mode tends to be smaller than in L-mode

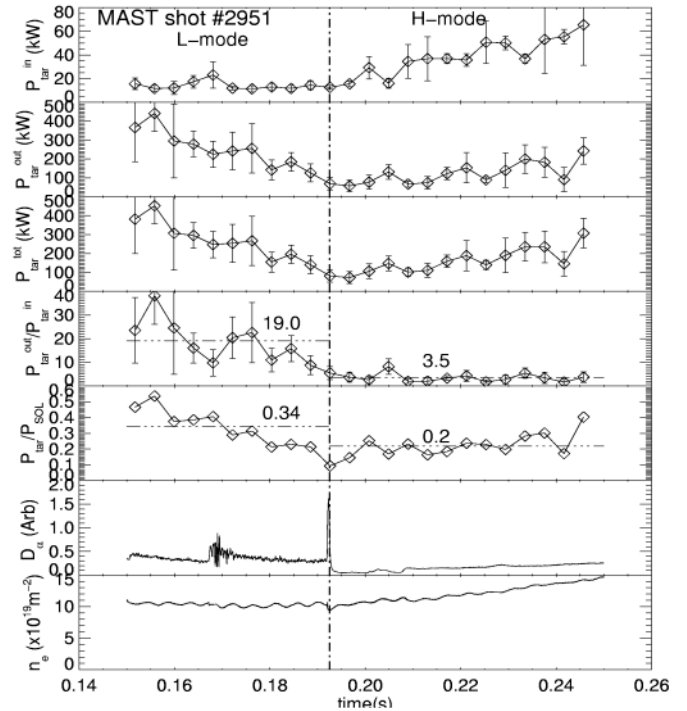


Fig.5 Power accounting results across L-H transition

to the ion channel with NBI heating, which is not detected using Langmuir probes, similar to observations on JET[3]. The DIVIMP modelling reveals that the T_i is approximately twice the T_e [2]. Since the probes only measure electron power, this may explain why only ~30% of P_{SOL} is measured at the target. Target thermography will be used to confirm this mechanism. This may also provide an explanation of why P_{tar} in H-mode is less than in L-mode although the core density rapidly increases after the L-H transition.

The ratio of total power to the outer and inner strike points in L-mode, average value of ~19, is far higher than that observed for Ohmic plasma, ~6, but falls to around 3~4 in H-mode (Fig 5), approximately equal to the ratio of outboard to inboard separatrix surface areas. The fall may be explained by a reduction in turbulent losses from the outboard side after the onset of H-mode (whereas the inboard side, which is at higher field and in a good curvature region, may be comparatively unaffected). In addition to the in-out asymmetries discovered above, there are also up-down asymmetries, which are even observed in a magnetically symmetric connected double null (CDN) configuration (eg, $P_{tar_{up}}:P_{tar_{down}} \sim 30:70$ at $t=177\text{ms}$ in the shot 3730 with downward ion grad B drift). The reason remains to be understood but the ExB drift effect could play a role. [4]

4. Conclusion

Measurements of the peak (strike-point) electron density, temperature and heat flux density at the inboard and outboard divertor targets have been made for NBI heated L and H-mode plasmas in the MAST tokamak. The plasmas are in collisional condition ($\nu_e^* > 6$, $\nu_i^* > 1.5$) at both inboard and outboard sides. There are significant differences in the plasma parameters between L and H-mode plasmas, causing higher (at the inboard) and lower (outboard) peak heat flux values after the transition to the H-mode. A relatively small fraction of power entering the SOL appears to flow to the target plates, less than 50% in L-mode and 30% in H-mode. The power ratio flowing to the outboard and inboard sides becomes much smaller (from ~19 to ~3.5) after the onset of H-mode. Up-down power asymmetry is observed even in a magnetically symmetric DND configuration, which may be driven by ExB poloidal drifts. The SOL data from MAST could be used for SOL width scaling studies to extrapolate to a future burning plasma machine such as an ST power plant or ITER.

Acknowledgements

This work is jointly funded by the UK Department of Trade and Industry and Euratom. One of the authors (J-W. Ahn) is supported by a grant from the British Foreign & Commonwealth Office.

References

- [1] J-W. Ahn, G.F.Counsell, J. Nucl. Mater. 290-293 (2001) 820-824.
- [2] A. Kirk, J-W.Ahn *et al*, 28th EPS Conf. on Contr. Fus. and Plas. Phys (2001)
- [3] W. Fundamenski *et al*, 28th EPS Conf. on Contr. Fus. and Plas. Phys (2001)
- [4] T.W. Petrie *et al*, J. Nucl. Mater. 290-293 (2001) 935-939